

Chapter 8

An Introduction to Quantum Field Theory

8.1 Introduction

This chapter is a generalization of the section on Path Integral Monte Carlo. Instead of considering one (or N) quantum-mechanical particles as was done there, the idea is now to consider a quantum *field*, which contains infinitely many degrees of freedom. However, in practice, we are going to simulate a large but finite number of degrees of freedom, and extrapolate at the end. So there really is not much difference with Sec. 5.1.

The formal basis for Quantum Field Theory is an important subject, which will not be covered here. The goal of this chapter is to convey some understanding of *simulations* of quantum field theories, by appealing to intuition rather than rigor.

8.2 Path integrals: from classical mechanics to field theory

Consider first the case of a single, classical particle with Hamiltonian $H = \frac{p^2}{2m} + V$. Hamilton's equations describe the time-evolution of this particle:

$$\frac{dq}{dt} = +\frac{\partial H}{\partial p} \longrightarrow \dot{q} = \frac{p}{m} \quad (8.1)$$

$$\frac{dp}{dt} = -\frac{\partial H}{\partial q} \longrightarrow \dot{p} = -\nabla V \quad (8.2)$$

The usual point of view is to start from initial conditions (q, \dot{q}) at time $t = 0$, and evolve q and \dot{q} according to the coupled ODEs above. Note, however, that the boundary conditions can instead be split between the beginning and the end of the evolution. In particular, one can specify the beginning and ending coordinates $(q(0), q(t))$. There is a unique path $q(t'), t' \in [0, t]$, which satisfies the above equations, and specifies the initial and final velocities. To find this path, it is convenient to change viewpoint and consider the action $S = \int_0^t dt' \mathcal{L}(q, \dot{q})$, where \mathcal{L} is the Lagrangian $\frac{1}{2}m\dot{q}^2 - V(q)$. One

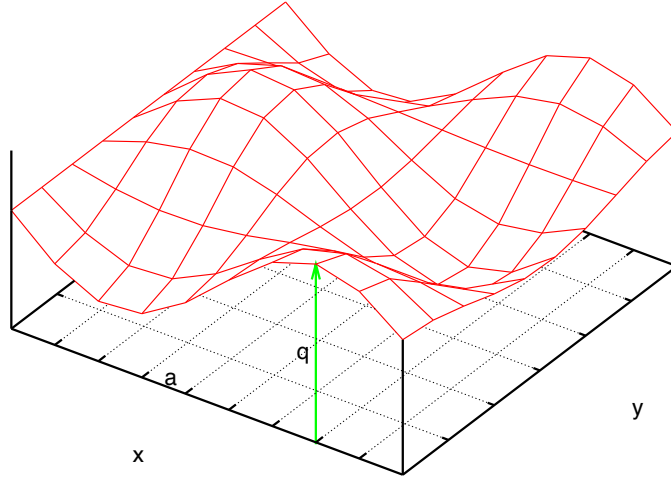


Figure 8.1: A field configuration $q(x, y)$, discretized on a square grid of spacing a .

then invokes the principle of stationary (or least) action, from which can be derived the Euler-Lagrange equations

$$\frac{\partial \mathcal{L}}{\partial q_i} = \partial_\mu \frac{\partial \mathcal{L}}{\partial (\partial_\mu q_i)} \quad . \quad (8.3)$$

Note that the notion of action is more general than the notion of Hamiltonian: some systems have an action, but no Hamiltonian. This was in fact the original motivation for Feynman to develop the path integral formalism in his Ph.D. thesis: he was interested in systems having non-local interactions in time (with an interaction term $q(t)q(t')$).

Consider now many particles interacting with each other, with Lagrangian $\mathcal{L} = \sum_i \frac{1}{2} m \dot{q}_i^2 - V(\{q_i\})$ and take q_i to represent the z -coordinate of particle i , whose x and y coordinates are fixed on a square grid of spacing a . Furthermore, take the interaction between particles to be of the form $\sum_{\langle ij \rangle} (q_i - q_j)^2$, where $\langle ij \rangle$ stands for nearest-neighbours on the grid, as if springs were connecting i and j . Low-energy configurations will then have almost the same q -value at neighbouring grid points, so that the configuration $\{q_i\}$ will be smooth and look like a “mattress” as in Fig. 8.1.

When the grid spacing a is reduced to zero, the configuration $\{q_i\}$ becomes a *classical field* $q(\vec{x})$ ($\vec{x} \in \mathcal{R}^2$ in this example), with infinitely many degrees of freedom. The action of this field is specified by its Lagrangian density $\mathcal{L} = \frac{1}{2} \partial_\mu q \partial^\mu q - \frac{1}{2} m_0^2 q^2 - V(q)$ where the first term is the continuum version of $(q_i - q_j)^2$ (with $\partial_\mu q \partial^\mu q = \dot{q}^2 - |\vec{\nabla} q|^2$), the second one is a harmonic term corresponding to a mass, and the last term describes the local (anharmonic) interaction, e.g. $\propto q^4$ ¹. The action is then $S = \int_0^t dt' dx dy \mathcal{L}(q(x, y, t'))$. Note that the Lagrangian density \mathcal{L} satisfies several symmetries: it is invariant under translations and rotations in the (x, y) plane, and under the sign flip $q(\vec{x}) \rightarrow -q(\vec{x}) \forall \vec{x}$, at least for an interaction $\propto q^4$. Each continuous symmetry leads to a conserved quantity: energy-momentum for translations, angular momentum for rotations. We will see the importance of the discrete symmetry $q \leftrightarrow -q$ later.

¹One could think of additional interaction terms, constructed from *higher derivatives* of the field. They are not considered here because they lead to non-renormalizable theories.

Now we can consider quantum effects on the above system. As a result of quantum fluctuations, the path from $q(t=0)$ to $q(t)$ is no longer unique. All paths contribute, with an amplitude $\propto \exp(-\frac{i}{\hbar} \int_0^t dt' \mathcal{L})$, from which it becomes clear that the magnitude of relevant fluctuations in the action is \hbar . One can then follow the strategy of Sec. 5.1 and make time purely imaginary, by introducing $\tau = -it \in \mathcal{R}$. The immediate result is that $-idt'$ above becomes $d\tau'$, so that the amplitude becomes real. The other change is $\dot{q}^2 \rightarrow -(\partial_\tau q)^2$, so that an overall minus sign can be taken out, leading to the amplitude

$$\exp(-\frac{1}{\hbar} S_E) \quad (8.4)$$

where $S_E = \int d\tau' d\vec{x} \mathcal{L}_E$ is the Euclidean action, and

$$\mathcal{L}_E = \frac{1}{2}(\partial_\mu \phi)^2 + \frac{1}{2}m_0^2 \phi^2 + V(\phi) \quad (8.5)$$

is the Euclidean Lagrangian density, and the field q is now denoted by ϕ as is customary. The first term $(\partial_\mu \phi)^2 = (\partial_\tau \phi)^2 + |\vec{\nabla} \phi|^2$ is now symmetric between space and time, so that the metric is *Euclidean* in $(d+1)$ dimensions (d spatial dimensions, plus “Euclidean” time).

It is worth summarizing the sign flips which occurred in the kinetic energy T and the potential energy U during the successive steps we have just taken. We started with the Hamiltonian $H = T + U$, then considered the Lagrangian $L = T - U$. Going to imaginary time changes the sign of T . Finally, we take out an overall minus sign in the definition of L_E , so that paths with the smallest action are the most likely. This leads to the Euclidean Lagrangian density $L_E = T + U$, which is identical to the Hamiltonian we started from, except that the momentum p is replaced by the derivative $\partial_0 \phi$.

It is also useful to perform some elementary dimensional analysis. Since it appears in the exponent of the amplitude Eq.(8.4), the Euclidean action S_E is *dimensionless* (we set $\hbar = 1$). Hence the Euclidean Lagrangian density has mass dimension $(d+1)$, and therefore the field ϕ has mass dimension $\frac{d-1}{2}$. This is interesting, because if we take the “normal” number of spatial dimensions $d = 3$ and the interaction term $V(\phi) = \frac{g_0}{4!} \phi^4$, then g_0 is a dimensionless number. It makes sense then to perform a Taylor expansion of this theory in powers of g_0 about the free case $g_0 = 0$: this is the scope of perturbation theory. Here, we will try to obtain non-perturbative results, by directly simulating the theory at some finite, large value of g_0 .

We have so far considered a field $\phi(\vec{x}, \tau)$ which takes values in \mathcal{R} . It is easy to generalize the Lagrangian density Eq.(8.5) to cases when ϕ takes values in \mathcal{C} , or has

several components forming a vector $\vec{\phi} \equiv \begin{pmatrix} \phi_1 \\ \dots \\ \phi_N \end{pmatrix}$, perhaps with a constraint $\sum_N \phi_k^2 =$

1, depending on the desired symmetries. Typically, the Euclidean Lagrangian density is the starting, defining point of a quantum field theory.

Finally, we can introduce a finite temperature T , exactly as we did in the quantum-mechanical case: we make the Euclidean time direction *compact*: $\tau \in [0, \beta = \frac{1}{T}]$, and impose periodic boundary conditions on the field ϕ : $\phi(\vec{x}, \beta) = \phi(\vec{x}, 0) \forall \vec{x}$. This works for the same reason as in quantum mechanics: the partition function

$$Z = \int_{\text{periodic}} \mathcal{D}\phi \exp(-\int_0^\beta d\tau' d\vec{x} \mathcal{L}_E(\phi)) \quad (8.6)$$

is a weighted sum of eigenstates of the Hamiltonian: $Z = \sum_i \exp(-\beta E_i)$. We will be concerned here with the $T = 0$ situation. In that case, the two-point correlator provides a means to measure the mass gap $(E_1 - E_0)$:

$$\langle \phi(\vec{x}, \tau) \phi(\vec{x}, 0) \rangle - \langle \phi \rangle^2 \underset{\tau \rightarrow \infty}{=} c^2 \exp(-(E_1 - E_0)\tau) \quad (8.7)$$

or equivalently the correlation length $\xi = (E_1 - E_0)^{-1}$. The lowest energy state, with energy E_0 , is the vacuum, which contains particle-antiparticle pairs because of quantum fluctuations, but whose net particle number is zero. The first excited state, with energy E_1 , contains one particle at rest. Call its mass $m_R = E_1 - E_0$. Then this mass can be obtained from the decay of the two-point correlator, as $m_R = 1/\xi$. This is the “true”, measurable mass of the theory, and it is not equal to the mass m_0 used in the Lagrangian density. m_R is called the *renormalized* mass, while m_0 is the *bare* mass. Similarly, the “true” strength g_R of the interaction can be measured from 4-correlators of ϕ , and it is not equal to the coupling g_0 used in the Lagrangian density: g_0 is the bare coupling, g_R the renormalized coupling.

8.3 Numerical study of ϕ^4 theory

Here, we show that very important results in Quantum Field Theory can be extracted from simulations of the $4d$ Ising model. Our starting point is the continuum Euclidean action:

$$S_E = \int d\tau d^3x \left[\frac{1}{2} (\partial_\mu \phi_0)^2 + \frac{1}{2} m_0^2 \phi_0^2 + \frac{g_0}{4!} \phi_0^4 \right] \quad (8.8)$$

where the subscript 0 is to emphasize that we are dealing with bare quantities (field, mass and coupling), and the coupling normalization $1/4!$ is conventional. We discretize the theory on a hypercubic ($4d$) lattice with spacing a ². After the usual replacements $\int d\tau d^3x \rightarrow a^4 \sum_{\text{sites } x}$ and $\partial_\mu \phi_0 \rightarrow \frac{\phi_0(x+\hat{\mu}) - \phi_0(x)}{a}$, we end up with the lattice action

$$S_L = \sum_x \left[-2\kappa \sum_\mu \phi(x) \phi(x + \hat{\mu}) + \phi(x)^2 + \lambda (\phi(x)^2 - 1)^2 - \lambda \right] \quad (8.9)$$

where we use the new variables ϕ, κ and λ defined by

$$a\phi_0 = \sqrt{2\kappa} \phi \quad (8.10)$$

$$a^2 m_0^2 = \frac{1 - 2\lambda}{\kappa} - 8 \quad (8.11)$$

$$g_0 = \frac{6\lambda}{\kappa^2} \quad (8.12)$$

Note in particular the multiplication of ϕ_0 by a to form a dimensionless variable, since ϕ_0 has mass dimension 1. The original formulation had two bare parameters, m_0 and g_0 . They have been mapped into two bare parameters, κ and λ . This discretized theory can be simulated by standard Monte Carlo algorithms like Metropolis, on a hypercubic

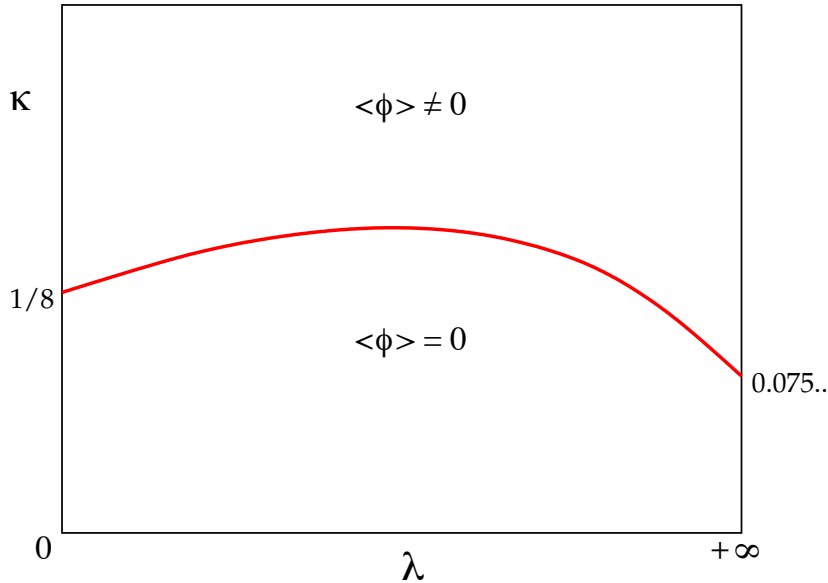


Figure 8.2: Phase diagram of the lattice theory defined by Eq.(8.9). The two phases are separated by a line of second-order transitions.

lattice of L sites in each direction. To minimize finite-size effects, periodic boundary conditions are usually imposed in each direction.

The behaviour of our system is easy to understand qualitatively in the two limits $\lambda = 0$ and $\lambda = +\infty$.

- When $\lambda = 0$, the interaction is turned off. This is the free theory, which has two phases depending on the value of κ : a disordered or symmetric phase $\langle \phi \rangle = 0$ when κ is small, and an ordered phase $\langle \phi \rangle \neq 0$ when κ is large. Thus, the symmetry $\phi \leftrightarrow -\phi$ is spontaneously broken when $\kappa > \kappa_c = \frac{1}{8}$, which corresponds to the vanishing of the mass m_0 .
- When $\lambda = +\infty$, fluctuations of ϕ away from the values ± 1 cost an infinite amount of energy. Thus, ϕ is restricted to ± 1 , and our theory reduces to the $4d$ Ising model with coupling 2κ . As in lower dimensions, the Ising model undergoes a *second-order phase transition* corresponding to the spontaneous breaking of the symmetry $\phi \leftrightarrow -\phi$, for a critical value $\kappa_c \approx 0.075$.

For intermediate values of λ , again a second-order transition takes place, leading to the phase diagram depicted Fig. 8.2.

The existence of a second-order phase transition is crucial: it allows us to define a *continuum limit* of our lattice theory. Remember that the “true”, renormalized mass m_R can be extracted from the exponential decay of the 2-point correlator

$$\langle \phi(x)\phi(y) \rangle - \langle \phi \rangle^2 \underset{|x-y| \rightarrow \infty}{\propto} \exp(-m_R|x-y|) = \exp\left(-\frac{|x-y|}{\xi}\right) \quad (8.13)$$

(see Eq.(8.7)). On the lattice, we can only measure the dimensionless combination

²The lattice spacing is taken to be the same in space and in time for simplicity; one could consider different values a_s and a_τ .

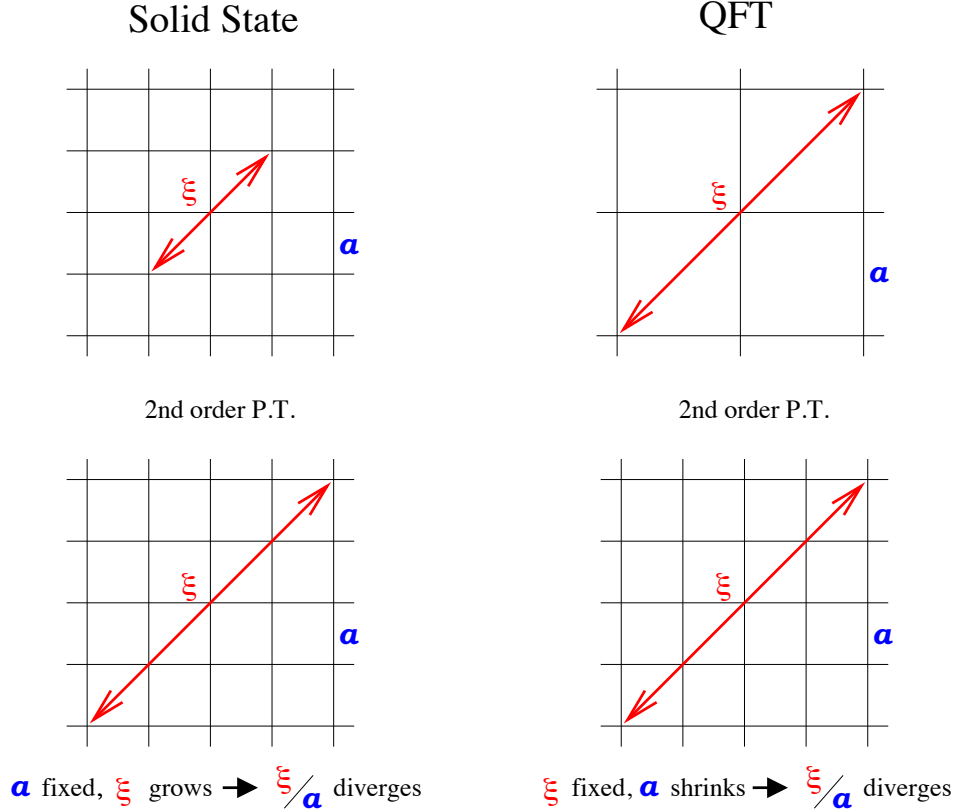


Figure 8.3: Two different viewpoints on a second-order phase transition: in solid-state physics (*left*), the crystal is “real” and the physical correlation length diverges; in quantum field theory (*right*), the correlation length is “real”, and the lattice spacing shrinks to zero.

$am_R = \frac{1}{\xi/a}$, and the separation $|x - y|$ can only be measured in lattice units, i.e. $\frac{|x-y|}{a}$. Taking the continuum limit $a \rightarrow 0$ (while keeping m_R fixed) forces the correlation length *measured in lattice units*, i.e. ξ/a , to diverge. This only occurs when the lattice theory has a second-order phase transition (or higher order).

Therefore, the interpretation of a second-order phase transition is different between solid-state physics and lattice field theory. In the first case, the lattice spacing has a physical meaning, like the distance between two ions in a crystal: the lattice is “for real”, and the correlation length really diverges at a second-order critical point. In the lattice field theory, the correlation length is “for real”, and the lattice spacing a shrinks to zero at the critical point. This is illustrated in Fig. 8.3.

In this latter case, one must be careful that the physical box size (La) also shrinks as $a \rightarrow 0$. In order to obtain a controlled continuum limit at constant physical volume, one must increase the number of lattice points L in each direction keeping (La) fixed.

Going back to our ϕ^4 theory, one sees that a continuum limit can be defined for any value of the bare coupling $\lambda \in [0, +\infty]$, by tuning κ to its critical value $\kappa_c(\lambda)$. An interesting question is: what is the value of the “true”, renormalized coupling as a function of λ ? The answer is clear when $\lambda = 0$: the theory is free, and the coupling is

zero, whether bare or renormalized. To obtain a non-zero answer, a reasonable strategy is to maximize the bare coupling, and thus to consider the Ising limit $\lambda = +\infty$. The renormalized coupling is extracted from the strength of the 4-spin correlation. The rather surprising answer is that the renormalized coupling is zero, just like for $\lambda = 0$. In fact, the renormalized coupling is always zero for any choice of λ . In other words, the renormalized ϕ^4 theory is *free*, no matter the value of the bare coupling! The formal statement is that the ϕ^4 theory is “trivial”. Note that this is only true in $(3 + 1)$ dimensions. In lower dimensions, the renormalized coupling is non-zero.

Now, why is this finding important? The Standard Model of particle interactions contains a Higgs particle, which gives a mass to all other particles by coupling to them. The field theory describing the Higgs particle is very much like the ϕ^4 theory we have just studied, except that the field ϕ is now a complex doublet $\begin{pmatrix} \phi_1 + i\phi_2 \\ \phi_3 + i\phi_4 \end{pmatrix}$. The bare parameters are chosen so that the system is in the broken-symmetry phase, where ϕ has a non-zero expectation value. The masses of all particles are proportional to $\langle\phi\rangle$, therefore it is crucial that $\langle\phi\rangle \neq 0$. In turn, this symmetry breaking is only possible if the coupling g is non-zero. But, as we have seen, the “true”, renormalized value of g is zero. Therefore, we have a logical inconsistency. The consequence is that the Standard Model cannot be the final, exact description of particle interactions. Some new physics beyond the Standard Model must exist, which becomes visible at an energy scale which depends on the Higgs boson mass. From the numerical study of the lattice theory near $\kappa_c(\lambda)$, one can set this scale at around 1000 GeV if the Higgs mass is around 600-800 GeV, or higher if the Higgs is lighter. In any case, the Higgs boson, and/or possibly new physics, must be found at energies ≤ 1000 GeV. This (slightly abridged) argument is so powerful that it has been used in the design of the Large Hadron Collider (LHC), turned on at CERN in 2009, and which will study collisions up to about 1000 GeV only.

8.4 Gauge theories

Of the four forces known in Nature, at least three (the strong, the weak and the electromagnetic forces) are described by gauge theories. In addition to the usual “matter” fields (electrons, quarks), these theories contain “gauge” fields (photons, W and Z bosons, gluons) which “mediate” the interaction: the interaction between, say, two electrons is caused by the exchange of photons between them. This is analogous to the exchange of momentum which occurs when one person throws a ball at another, and the other catches it. In this way, two particles interact when they are far apart, even though the Lagrangian contains only local interactions. Moreover, gauge theories are invariant under a larger class of symmetries, namely *local* (x -dependent) symmetries.

8.4.1 QED

As an example, let us consider here a variant of Quantum ElectroDynamics (QED), called scalar QED, where electrons are turned into bosons. A simple modification of the previous ϕ^4 theory is required: in order to represent charged bosons, the field ϕ , instead of being real, is made complex, $\phi(x) \in \mathcal{C}$. The continuum Euclidean action

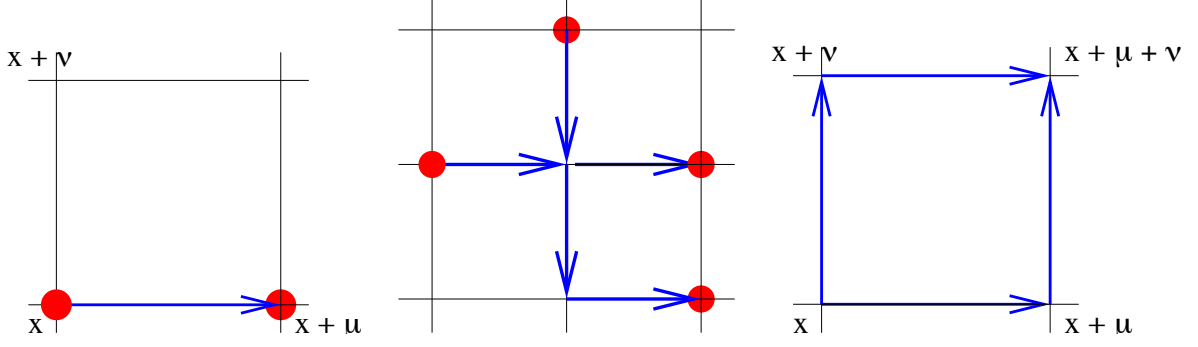


Figure 8.4: Graphical representation (*left*) of the gauge-invariant nearest-neighbour interaction: $\phi^*(x)\phi(x + \hat{\mu})$ becomes $\phi^*(x)U_\mu(x)\phi(x + \hat{\mu})$; (*middle*) an example of a gauge-invariant 4-point correlation; (*right*) the smallest closed loop is the plaquette, with associated matrix $U_\mu(x)U_\nu(x + \hat{\mu})U_\mu^\dagger(x + \hat{\nu})U_\nu^\dagger(x)$.

becomes

$$S_E = \int d\tau d^3x \left[|\partial_\mu \phi_0|^2 + m_0^2 |\phi_0|^2 + \frac{g_0}{4!} |\phi_0|^4 \right] \quad (8.14)$$

and, after discretization on the lattice:

$$S_L = \sum_x \left[-\kappa \sum_\mu (\phi^*(x)\phi(x + \hat{\mu}) + \text{h.c.}) + |\phi(x)|^2 + \lambda(|\phi(x)|^2 - 1)^2 - \lambda \right] \quad (8.15)$$

S_L is invariant under the *global* (x -independent) rotation $\phi(x) \rightarrow \exp(i\alpha)\phi(x) \forall x$. The idea is now to promote this symmetry to a *local* one, where α may depend on x . It is clear that the derivative term $\phi^*(x)\phi(x + \hat{\mu})$ is not invariant under this transformation. Invariance is achieved by introducing new degrees of freedom, namely complex phases (elements of $U(1)$) which live on the links between nearest-neighbours. Call $U_\mu(x) = \exp(i\theta_\mu(x))$ the link variable starting at site x in direction μ . Modify the derivative term as follows:

$$\phi^*(x)\phi(x + \hat{\mu}) \rightarrow \phi^*(x)U_\mu(x)\phi(x + \hat{\mu}) \quad (8.16)$$

This term is now invariant under a *local* transformation $\phi(x) \rightarrow \exp(i\alpha(x))\phi(x)$, with $\alpha(x) \neq \alpha(x + \hat{\mu})$, provided that $U_\mu(x)$ also transforms:

$$\phi(x) \rightarrow \exp(i\alpha(x))\phi(x) \quad (8.17)$$

$$U_\mu(x) \rightarrow \exp(i\alpha(x))U_\mu(x)\exp(-i\alpha(x + \hat{\mu})) \quad (8.18)$$

The significance of the new variables $U_\mu(x)$ and of the new expression for the discretized derivative can be elucidated by expressing $\theta_\mu(x) = eaA_\mu(x)$, and considering the continuum limit $a \rightarrow 0$. To lowest order in a , the derivative ∂_μ becomes the *covariant derivative* $D_\mu \equiv \partial_\mu + ieA_\mu$, and the transformation eq.(8.18) is a *gauge transformation* for A_μ : $A_\mu(x) \rightarrow A_\mu(x) - e\partial_\mu\alpha(x)$. Thus, our link variables $U_\mu(x)$ represent the discretized gauge potential $A_\mu(x)$ associated with the electromagnetic field, and eq.(8.16) describes the interaction of our bosonic electrons with the photon. To complete the discretization of QED, what is missing is the energy of the electromagnetic field, namely $\frac{1}{2} \int d\vec{x} d\tau (|\vec{E}|^2(x) + |\vec{B}|^2(x))$. We identify its lattice version below.

It becomes simple to construct n -point correlators of ϕ which are invariant under the local transformation eq.(8.18): all the fields ϕ need to be connected by “strings” of gauge fields, made of products of gauge links U_μ as in Fig. 8.4. Under a local gauge transformation, the phase changes $\alpha(x)$ will always cancel out between ϕ and the attached U , or between two successive U 's.

There is another type of gauge-invariant object. Consider the product of links $\prod_{x \rightarrow x} U$ around a closed loop, starting and ending at x . It transforms as

$$\prod_{x \rightarrow x} U \rightarrow \exp(i\alpha(x)) \prod_{x \rightarrow x} U \exp(-i\alpha(x)) \quad (8.19)$$

which is invariant since all the U 's are complex phases which commute with each other. Thus, another valid term to add to the [real] lattice action is the real part of any closed loop, summed over translations and rotations to preserve the other desired symmetries. The simplest version of such a term is to take elementary square loops of size a , made of 4 links going around a *plaquette*: $P_{\mu\nu}(x) \equiv U_\mu(x)U_\nu(x + \hat{\mu})U^\dagger(x + \hat{\mu})U^\dagger(x)$. Thus, the complete action of our scalar QED theory is

$$\sum_x |\phi(x)|^2 - \kappa \sum_x \sum_\mu (\phi^*(x)U_\mu(x)\phi(x + \hat{\mu}) + \text{h.c.}) + \beta \sum_x \sum_{\mu \neq \nu} \text{Re}(P_{\mu\nu}(x)) \quad (8.20)$$

The plaquette term looks geometrically like a curl. Indeed, substituting $U_\mu(x) = \exp(ieaA_\mu(x))$ and expanding to leading-order in a yields

$$\text{Re}(P_{\mu\nu}(x)) \approx 1 - \frac{1}{2}e^2a^4(\partial_\mu A_\nu - \partial_\nu A_\mu)^2 \quad (8.21)$$

so that the last term in eq.(8.20) becomes, up to an irrelevant constant, $-\beta e^2 \frac{1}{2} \int d\vec{x} d\tau (|\vec{E}|^2 + |\vec{B}|^2)$, where one has expressed the electric and magnetic fields \vec{E} and \vec{B} in terms of the gauge potential A_μ . It suffices then to set $\beta = 1/e^2$ to recover the energy of an electro-magnetic field.

Note that it is our demand to preserve invariance under the local transformation eq.(8.18) which has led us to the general form of the action eq.(8.20). We could have considered larger loops instead of plaquettes. But in the continuum limit $a \rightarrow 0$, these loops would yield the same continuum action. So the form of the QED action is essentially dictated by the local gauge symmetry.

One can now study the scalar QED theory defined by eq.(8.20) using Monte Carlo simulations, for any value of the bare couplings (κ, β) . Contrary to continuum perturbation theory, one is not limited to small values of e (i.e. large β).

8.4.2 QCD

Other gauge theories have basically the *same* discretized action eq.(8.20). What changes is the group to which the link variables $U_\mu(x)$ belong. For QCD, these variables represent the gluon field, which mediates the interaction between quarks. Quarks come in 3 different colors and are thus represented by a 3-component vector at each site³. Hence,

³This would be the full story if quarks were bosons. Because they are fermions, each color component is in fact a 4-component vector, called Dirac *spinor*.

the link variables are 3×3 matrices. The gauge-invariant piece associated with a closed loop is the *trace* of the corresponding matrix, thanks to cyclic invariance of the trace of eq.(8.19). No other changes are required to turn lattice QED into lattice QCD!

As emphasized in Sec. 8.3, the Euclidean Lagrangian density defines the lattice theory. The continuum limit can be obtained by approaching a critical point. For QCD, the critical point is $\beta \rightarrow +\infty$, i.e. $g_0 = 0$ since $\beta \propto 1/g_0^2$ as in QED. As we have seen, the vanishing of the bare coupling does not imply much about the true, renormalized coupling.

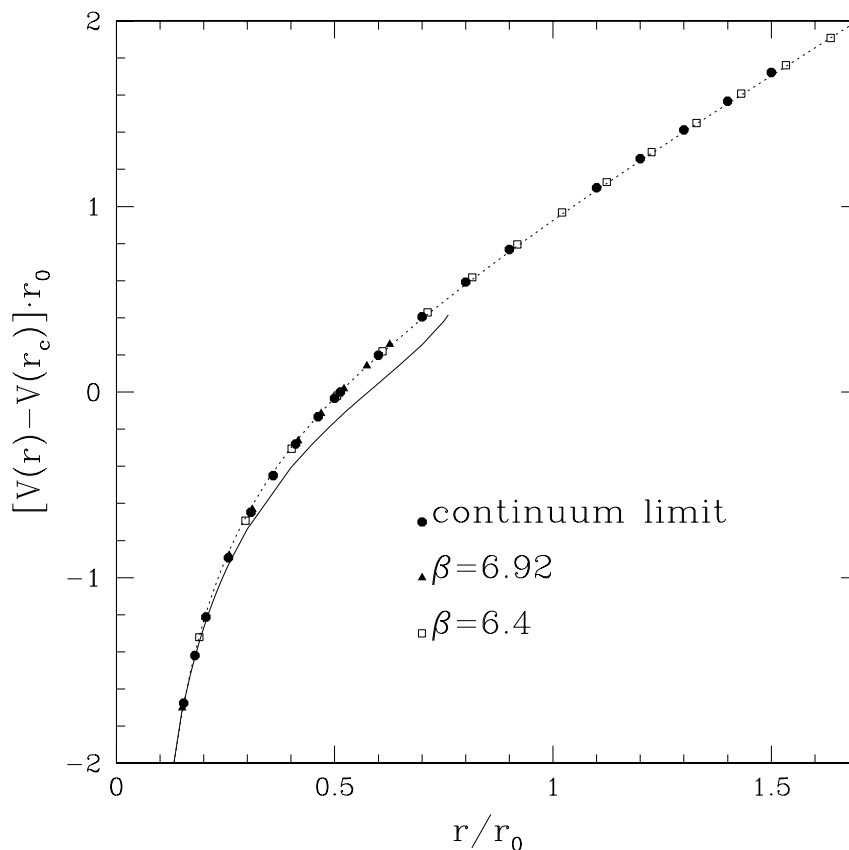


Figure 8.5: Potential $V(r)$ between a static quark and antiquark, as a function of their separation r . Data obtained at 2 values of the lattice spacing (finite values of β) are extrapolated to the continuum limit ($\beta \rightarrow \infty$). At short distance, the potential is Coulomb-like because the interaction becomes weak (the solid line shows the prediction of perturbation theory). At large distance, the potential rises linearly, which shows that it takes an infinite energy to separate the two objects: quarks are confined. A simple model of a vibrating string (dotted line) gives a good description, down to rather short distances. From *hep-lat/0108008*.

8.5 Overview

The formulation of lattice QCD is due to K. Wilson (1974). First Monte Carlo simulations were performed by M. Creutz in 1980, on a 4^4 lattice. A goal of early simulations was to check whether quarks were confined. This can be demonstrated by considering the potential $V(r)$ between a quark and an anti-quark separated by distance r . Contrary to the case of QED where the potential $\propto 1/r$ saturates as $r \rightarrow \infty$, in QCD the potential keeps rising linearly, $V(r) \sim \sigma r$, so that it takes an infinite amount of energy to completely separate the quark and anti-quark. Equivalently, the force between the two objects goes to a *constant* σ . The energy of the quark-antiquark pair grows as if it was all concentrated in a tube of finite diameter. Describing the quark-antiquark pair as an infinitely thin, vibrating string is a very good approximation, as shown in the state-of-the-art Monte Carlo data Fig. 8.5, now performed on 32^4 lattices. To control discretization errors, the lattice spacing must be about $1/10^{\text{th}}$ of the correlation length or less. To control finite-volume effects, the lattice size must be about 3 times the correlation length or more. This implies lattices of minimum size 30^4 , which have only become within reach of a reasonable computer budget in recent years.

The above simulations considered only the effect of gluons: since gluons carry a color charge (in contrast to the photon which is electrically neutral), they can lead to complex effects like the confinement of charges introduced in the gluon system. But to study QCD proper, quarks must be simulated also. This is more difficult because quarks are fermions, i.e. non-commuting variables. The strategy is to integrate them out analytically. This integration induces a more complicated interaction among the remaining gluonic link variables. In fact, this interaction is *non-local*, which increases the algorithmic complexity of the Monte Carlo simulation. An efficient, exact simulation algorithm, called Hybrid Monte Carlo, was only discovered in 1987 (see bibliography). Even so, the simulation of so-called “full QCD”, on lattices of size 30^4 or larger, requires a computer effort $\mathcal{O}(1)$ Teraflop \times year, which has forced the community to evolve into large collaborations using dedicated computers.

Using these resources, one is now able to reproduce the masses of quark and anti-quark bound states, i.e. mesons and baryons, to a few percent accuracy. The impact of neglecting the effect of quarks or including them is nicely illustrated in Fig. 8.6. Some predictions have also been made for the properties of mesons made of charm or bottom quarks, currently being studied in particle accelerators.

Another essential purpose of QCD simulations is to quantify QCD effects in experimental tests of the electroweak Standard Model. By checking whether experimental results are consistent with the Standard Model, one can expose inconsistencies which would be the signature of new, beyond-the-standard-model physics. To reveal such inconsistencies, one must first determine precisely the predictions of the Standard Model. This entails the determination of QCD effects, which can only be obtained from lattice QCD simulations.

Finally, another direction where QCD simulations have been playing a major role is that of high temperature. The confinement of quarks, which is an experimental fact at normal temperatures, is believed to disappear at very high temperatures $\mathcal{O}(100)$ MeV $\sim \mathcal{O}(10^{12})$ K. This new state of matter, where quarks and gluons form a plasma, is being probed by accelerator experiments which smash heavy ions against each other.

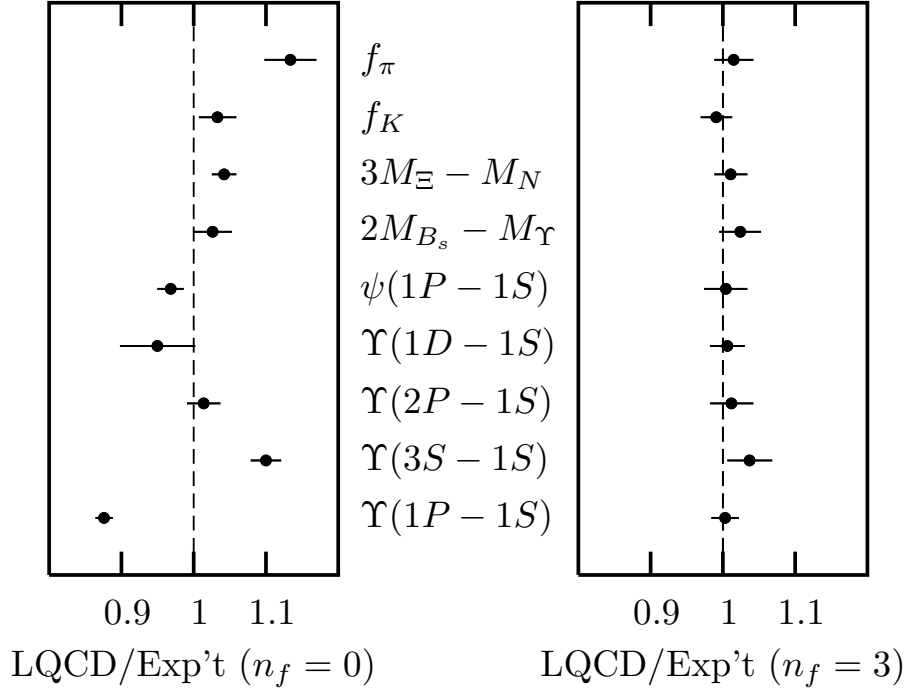


Figure 8.6: Comparison of lattice and experimental measurements of various quantities. The left figure shows the ratios lattice/experiment, for a lattice model which neglects quark effects (the number n_f of quark flavors is set to zero). The right figure shows the same ratios, for a lattice model including 3 quark flavors, all with equal masses. From *hep-lat/0304004*.

Lattice simulations provide an essential tool to predict the properties of this plasma.

8.6 Useful references

- *Computational Physics*, by J.M. Thijssen, Cambridge Univ. Press (2007), second edition. See Chapter 15.
- *Quantum Field Theory in a nutshell*, by A. Zee, Princeton Univ. Press (2003). This book reads like a thriller.
- *Hybrid Monte Carlo*, by S. Duane, A. D. Kennedy, B. J. Pendleton and D. Roweth, Phys. Lett. B **195** (1987) 216.